NIH Public Access
Author Manuscript
Eur J Nucl Med Mol Imaging. Author manuscript; available in PMC 2008 June 1.

Published in final edited form as:
Eur J Nucl Med Mol Imaging. 2008 June ; 35(6): 1192–1203.

Biodisposition and metabolism of [^{18}F]fluorocholine in 9L glioma cells and 9L glioma-bearing Fisher rats

Aditya Bansal, MS[1], **Wang Shuyan, MD**[2], **Toshiko Hara, MD, Ph.D.**[2], **Robert A. Harris, Ph.D.**[1], and **Timothy R. DeGrado, Ph.D.**[1,2]

1 *Department of Biochemistry and Molecular Biology, Indiana University School of Medicine, Indianapolis, IN*

2 *Department of Radiology, Indiana University School of Medicine. Indianapolis, IN*

Abstract

Purpose—[^{18}F]Fluorocholine [^{18}F]FCH) was developed as an analog of [^{11}C]choline for tumor imaging, however, its metabolic handling remains ill-defined. In this study, the metabolism of [^{18}F]FCH is evaluated in cultured 9L glioma cells and Fisher 344 rats bearing 9L glioma tumors.

Methods—9L glioma cells were incubated with [^{18}F]FCH and [^{14}C]choline under normoxic and hypoxic (1% O_2) conditions and analyzed for metabolic fate. [^{18}F]FCH and [^{14}C]choline kinetics and metabolism were studied in Fisher 344 rats bearing subcutaneous 9L tumors.

Results—[^{18}F]FCH and [^{14}C]choline were similarly metabolized in 9L cells in both normoxic and hypoxic conditions over a 2 hr incubation period. In normoxia, radioactivity was predominantly in phosphorylated form for both tracers after 5 min incubation. In hypoxia, the tracers remained mainly in nonmetabolized form at early timepoints (< 20 min). Slow dephosphorylation of intracellular [^{18}F]phosphofluorocholine (0.043–0.060 min^{-1}) and [^{14}C]phosphocholine (0.072–0.088 min^{-1}) was evidenced via efflux measurements. In rat, both [^{18}F]FCH and [^{14}C]choline showed high renal and hepatic uptake. Blood clearance of both tracers was rapid with oxidative metabolites, [^{18}F]fluorobetaine and [^{14}C]betaine, representing the majority of radiolabel in plasma after 5 min post-injection. Oxidation (in liver) and lipid incorporation (in lung) were somewhat slower for [^{18}F]FCH relative to [^{14}C]choline. The majority of radiolabel in hypoxic subcutaneous tumor, as in hypoxic cultured 9L cells, was found as nonmetabolized [^{18}F]FCH and [^{14}C]choline.

Conclusions—[^{18}F]FCH mimics choline uptake and metabolism by 9L glioma cells and tumors. However, subtle changes in biodistribution, oxidative metabolism, dephosphorylation, lipid incorporation and renal excretion show moderate effects of the presence of the radiofluorine atom in [^{18}F]FCH. The decrease in phosphorylation of exogenous choline by cancer cells should be considered in interpretation of PET images in characteristically hypoxic tumors.

Keywords

choline; fluorocholine; ^{18}F; 9L glioma; rat; metabolism; hypoxia

Corresponding Author's Contact Information: Dr. Timothy R. DeGrado, Indiana University School of Medicine, 1345 West 16th Street, L-3 Rm 202, Indianapolis, IN 46202-2111, Tel. 317-278-0029, FAX 317-278-9711, e-mail: tdegrado@iupui.edu.

Conflict of Interest Statement
No authors have affiliations that present conflicts of interest for this work.

NIH-PA Author Manuscript
NIH-PA Author Manuscript
NIH-PA Author Manuscript

NIH-PA Author Manuscript

NIH-PA Author Manuscript

NIH-PA Author Manuscript

Introduction

In recent years, alterations of choline uptake and metabolism have come to be recognized as hallmarks of malignancy [1]. High choline uptake and increased choline kinase activity have been reported in many cancers [2–5]. Choline kinase is known to be over-expressed in lung, colorectal, and prostate cancers [6]. The potential for PET imaging using [^{11}C]choline has been shown in detection of brain tumor [7,8], prostate carcinoma [9], and esophageal carcinoma [10]. However, the short half-life of [^{11}C]choline ($T_{1/2}$ = 20 min) limits its use to facilities that have a cyclotron within a short distance from the imaging suite. To allow for more practical distribution of a longer-lived tracer, the ^{18}F-labeled choline analog ($T_{1/2}$ = 109 min), [^{18}F] fluorocholine ([^{18}F]FCH) was developed [2,11]. Preliminary studies have shown [^{18}F]FCH to be a promising PET imaging tracer for prostate cancer, hepatocellular carcinoma and brain tumor imaging [11–19]. However, there is lacking an understanding of the influence of the fluorine atom in [^{18}F]FCH on its biodisposition and metabolism, and how its biochemical properties impact the interpretation of the imaging data. Previous work with radiolabeled cholines suggested the importance of the Kennedy pathway beginning with phosphorylation as well as oxidation to betaine (Figure 1) [20]. Therefore, in this study, our primary objective was to compare [^{18}F]FCH and radiolabeled choline with respect to their uptake and metabolism in a tumor-bearing rodent model. To allow access to multiple blood samples for metabolic analysis in a well-characterized tumor model, the 9L glioma bearing Fisher 344 rat model was chosen. Since it is known that subcutaneous 9L tumors are hypoxic [21], we sought to clarify the observations in the 9L tumors by undertaking metabolic studies with the choline radiotracers in normoxic and hypoxic cultured 9L cells. On the basis of structural similarity, we anticipated that [^{18}F]FCH would mimic choline uptake and metabolism in cultured cancer cells, normal tissue, and 9L tumors in rat, resulting in physiologic processing similar to choline. Thus, the purpose of this study was to utilize the 9L glioma-bearing rat model to clarify the metabolic handling of [^{18}F]FCH relative to radiolabeled choline, and to clarify the effects of hypoxia on the choline tracer's uptake and metabolism through analytical studies.

Materials and Methods

Male Fisher CDF 344 rats were obtained from Charles River Laboratories International, Inc., (Wilmington, MA). 9L glioma cells were from ATCC (Manassas, VA). [^{14}C]choline (370 MBq/mmol), HEPES, Tris, NaCl, KCl, $CaCl_2$, $MgCl_2$, glucose, choline, sodium pentobarbital, phosphate buffered saline (PBS), ATP, perchloric acid, NADP, hexokinase, glucose-6-P dehydrogenase, urea, phosphocreatine, creatine phosphokinase, DOWEX resin, heparin, EGTA, DTT, benzamidine, EDTA, HEPES, triton X-100, Bovine Adult Serum, N-tosyl-L-phenylalanine chloromethyl ketone (TPCK), trypsin inhibitor, PMSF leupeptin, and antipain were obtained from SIGMA (St. Louis, MO). [^{3}H]choline (3330 GBq/mmol) was obtained from Perkin Elmer Life Sciences (Wellesley, MA), [18F]FCH was synthesized according to method described by DeGrado et al [2,11]. The specific activity of [^{18}F]FCH was greater than 200 GBq/μmol as determined using electrospray ionization mass spectrometry (Thermo Scientific LTQ, Waltham, MA). All other chemicals were obtained from Fisher Scientific International Inc. (Hampton, NH). Modular incubator chamber was obtained from Billups-Rothenberg, Del Mar, CA. Hypoxic gas mixture (5% CO_2, 1%O_2, 94% N_2) was from Bioblend PraxAir, San Ramon, CA. A Wallac 1480 gamma counter was used for counting ^{18}F-radioactivity and Beckman Coulter LS6500 scintillation counter was used to count ^{14}C-radioactivity. Z1 Coulter particle Counter and Z-Pack Balanced electrolyte solution was from Beckman Coulter, Fullerton, CA. Dulbecco's modified Eagle's medium (DMEM) and fetal bovine serum were from ATCC (Manassas, VA). Trypsin was obtained from Mediatech Inc. (Herndon, VA).

NIH-PA Author Manuscript

NIH-PA Author Manuscript

NIH-PA Author Manuscript

Uptake and metabolism in cultured 9L glioma cells

Studies of tracer choline uptake were performed in cultured 9L glioma cells in normoxic and hypoxic conditions. For the latter condition, a 24 h exposure to hypoxia (1% O_2) was chosen as a preconditioning period before administration of choline radiotracers because significant changes in protein expression are seen only during prolonged (>16 h) hypoxic (1% O_2) exposure [22]. Furthermore, in our experience, 9L glioma cells are viable under hypoxia (1% O_2) for 48 h. Sub-confluent cultures of 9L glioma cells were placed under a humidified normoxic gas mixture (21% O_2, 75% N_2, 5% CO_2) or a hypoxic gas mixture (1% O_2, 94% N_2, 5% CO_2). After 24h incubation at 37°C, the cells were then incubated with [^{14}C]choline or [^{3}H]choline and [^{18}F]FCH for 5 min and 20 min. Exposure to respective gas mixture was maintained throughout the experiment. Uptake studies were done in DMEM supplemented with 10% fetal bovine serum in triplicate in 6 well plates. The medium contained 28 μM choline (physiological range 10–30 μM, ~ 74 KBq [^{14}C]choline or [^{3}H]choline and ~ 370 KBq [^{18}F]FCH per well. After incubation with the radiotracers, the cells were lysed in 1 ml of 0.3 N NaOH and 1% SDS and the total cellular radioactivity was determined by gamma and scintillation counting. ^{18}F-radioactivity was counted using a gamma counter on the same day. After decay of ^{18}F, scintillation fluid was added to the samples and they were counted for ^{14}C-radioactivity using a liquid scintillation counter.

For metabolite analysis, the cells were incubated with ~ 444 KBq [^{14}C]choline or [^{3}H]choline and ~ 1.85 MBq [^{18}F]FCH per well. At the end of incubation, the cells were washed 3 times with chilled phosphate buffered saline (PBS). For metabolite analysis, the cells were scraped in 500 μl chloroform/methanol (2:1) and sonicated at 4 °C. To the sonicated cell suspension was added 100 μl aqueous urea (40%) and 100 μl sulfuric acid (5%). The cells were sonicated for another 15 s, and then centrifuged at 2,500 g for 5 min at 4 °C. Hydrophilic choline metabolites in the aqueous layer were analyzed using gradient HPLC as described below. Aqueous and organic fractions were separated and counted.

To enhance cellular uptake of choline tracer and the potential production of oxidative metabolites, cells were incubated for 2 h using HEPES/Tris buffer (20 mM HEPES/Tris pH 7.4, 1 mM NaCl, 4 mM KCl, 2.8 mM $CaCl_2$, 1 mM $MgCl_2$, and 10 mM glucose) containing lower concentration of choline (10 μM). To rule out the possibility of auto-oxidation of choline, a stability test was done by incubating ~ 444 KBq [^{3}H]choline in HEPES-Tris buffer for 1 h. Equal amount of chloroform/methanol (2:1) was added to the buffer and centrifuged at 2500g for 5 min to separate aqueous fraction. Hydrophilic choline metabolites in the aqueous layer were analyzed using HPLC.

Cell counting and calculation of doubling time

Cell counts and cell doubling time were measured in parallel with the previously described tracer studies. Cells were trypsinized and suspended in a known volume of medium. The cell suspension was diluted 1000 fold with balanced electrolyte solution. Cells were counted in the diluted suspension using a particle counter. Doubling time was calculated using the formula DT (days) =T x 0.693 / ln (Nf / Ni), where DT is time needed to double a cell population, T is the incubation time in days, Ni is the cell number at the beginning of the incubation time and Nf is the cell number at the end of the incubation time. The uptake measurements were normalized to one million cells based on these cell count data.

Pulse-chase experiment

To investigate the efflux rates of radioactivity from 9L glioma cells after initial uptake, a pulse-chase experiment was performed. After 24 h incubation at 37°C under normoxic or hypoxic conditions, the 9L glioma cells were incubated with [^{14}C]choline and [^{18}F]FCH for 2 h at 37° C under similar conditions. The cells were then washed with PBS and incubated in fresh

NIH-PA Author Manuscript

NIH-PA Author Manuscript

NIH-PA Author Manuscript

medium. The cycle of washing and incubation was repeated every 15 min over a 2 h period. Radioactivity was counted in the PBS washes and the incubation medium after each cycle. The PBS washes and the fresh medium were equilibrated with 21% O_2 (normoxic condition) or 1 % O_2 (hypoxic condition). Hydrophilic choline metabolites in the washout were analyzed using HPLC.

ATP measurement

ATP concentrations in cultured cells were determined from neutralized perchloric acid cell extracts by a spectrophotometric method [23].

Choline kinase assay

The cells were scraped and homogenized in chilled extraction buffer pH 7.5 (30 mM HEPES pH 7.5, 3% Triton X-100, 2 mM EDTA, 2 % Bovine Adult Serum, 10 μM N-tosyl-L-phenylalanine chloromethyl ketone (TPCK), 10 mg/ml trypsin inhibitor, 1 μM leupeptin, 0.75 mg/ml DTT, 0.4 mg/ml PMSF). The cell homogenate was centrifuged for 10,000 g for 20 min at 4 °C. The supernatant was used for the assay as described by Ishidate and Nakazawa [24]. The assay mixture (300 μl) contained 0.1 M Tris-HCl, pH 7.5, 10 mM ATP, 12 mM $MgCl_2$, 100 μM choline, [^{14}C]choline (~0.7 MBq / assay mixture). Samples were incubated at 37 °C for 30 min.

Biodistribution and metabolite study in 9L glioma tumor bearing rat tumor model

The 9L glioma-bearing rat model was chosen for in vivo studies of [^{18}F]FCH metabolism because it is a well-characterized tumor model (2) and serial blood sampling for metabolite analysis is practical. Male Fisher CDF 344 rats (~ 200 g) were anesthetized with sodium pentobarbital (45 mg/kg IP). The thigh area was shaved and 2–3 x 10^6 cultured 9L glioma cells suspended in 50 μl PBS were inoculated under the skin. The tumor was allowed to grow to the size of approximately 1.5 cm^3 (about 4 weeks). Prior to radiotracer administration, the rat was placed on a warming pad (37°C), a femoral cut-down was performed, and a femoral vein catheter was established for injection of radiotracers. The neck area was incised and a carotid catheter was established (~50 μl volume pre-filled with heparin and plugged at the end). The rat was heparinized by venous injection of 28 units heparin in 50 μl isotonic saline.

Groups of animals (n = 4 each) were studied after bolus intravenous administration of [^{18}F] FCH (74 MBq) and [^{14}C]choline (1.8 MBq) in isotonic saline. Blood samples were collected from the carotid artery at a rate of 2 samples / min over the first 5 min and 1 sample / 5 min thereafter. At 5 or 20 min after bolus injection, rats were euthanized and tissues excised for radioactivity counting and metabolite analysis. Lung, liver, kidney and tumor tissue samples were rinsed in chilled saline and blotted to remove excess liquid. A portion of each tissue was weighed and counted for ^{18}F-radioactivity, while the remainder was used for metabolite analysis. The remaining tissues (brain, heart, skeletal muscle, small and large intestines, bone, colon, prostate, and skin) were rinsed in chilled saline, blotted to remove excess liquid, weighed and counted for ^{18}F-radioactivity. Urine samples were withdrawn from the bladder with a syringe. Blood samples were centrifuged, and the plasma was separated and counted. ^{18}F-radioactivity in the tissue and plasma samples was allowed to decay for at least 24 h before counting for ^{14}C-radioactivity. Tissues were incubated with 0.5 ml tissue solubilizer (SOLVABLE, Perkin Elmer) at 37 °C overnight, 5 ml scintillation cocktail was added, and ^{14}C-radioactivity was counted.

Analysis of radiolabeled metabolites

Tissue samples were homogenized using a polytron homogenizer in 5 ml chloroform/methanol (2:1) at 4 °C. The homogenate was sonicated for 15 s, then 1 ml aqueous urea (40%) and 1 ml

NIH-PA Author Manuscript

NIH-PA Author Manuscript

NIH-PA Author Manuscript

sulfuric acid (5%) was added. The suspension was sonicated for another 15 s. The suspension was centrifuged at 2,500 g for 5 min. Aqueous and organic fractions were separated and counted. Plasma samples were worked up as described above for tissue without homogenization. Samples of the aqueous phase were applied to an Adsorbosphere Silica HPLC column (4.6 x 250 mm, 10 μ) (Alltech Associates, Deerfield, IL). The following gradient was used for the HPLC separation: Solvent B in the eluent: 0% at 0–3 min, 0–30% at 3–10 min, 30–40% at 10–20 min, 40–100% at 20–22 min, 100% at 22–50 min, 100-0% 50–56 min, and 0% at 56–57 min. Solvent A was acetonitrile/water/ethanol/ 1M ammonium acetate/glacial acetic acid (0.8/0.127/0.068/0.003/0.002 (v/v)) and Solvent B was acetonitrile/water/ethanol/ 1M ammonium acetate/glacial acetic acid (0.44/0.44/0.085/0.027/0.018 (v/v)). The HPLC eluant was collected in 1-min fractions. Based on their retention time, the metabolites phosphocholine (31 min), phosphoryl-[^{18}F]FCH (28 min), choline (16 min), betaine (11 min), [^{18}F]FCH (13 min) and [^{18}F]fluorobetaine (8 min) were identified in the fractions. Retention times were determined using unlabeled standards of choline, FCH, betaine, fluorobetaine, phosphocholine and phosphoryl-FCH and mass-spectrometry detection (Varian, Palo Alto, CA). ^{18}F-radioactivity in 100 μl standard of injectate and collected samples were measured in gamma counter. The samples were then allowed to decay for at least 24 h. The injectate and samples in a liquid scintillation counter were counted for ^{14}C-radioactivity.

Statistical analysis

The data were compared using paired or unpaired t-test analyses as appropriate. Differences were regarded as statistically significant for $p<0.05$.

Results

Cultured 9L glioma cells

In normoxic 9L glioma cells incubated with radiolabeled choline and [^{18}F]FCH, the choline tracers were taken up avidly, and rapidly phosphorylated (Figure 2 and Table 1). The fraction of aqueous soluble radioactivity in the form of phosphocholine was 83%, 95% and 99% for incubation periods of 5, 20, and 120 min, respectively. By 2 hr incubation, approximately 19% of the radioactivity was associated with lipophilic metabolites. Uptake of [^{18}F]FCH by 9L glioma cells over a 2-h period was similar to that of radiolabeled choline (Figure 2 and Table 1). Furthermore, there were no significant differences in the levels of radiolabeled metabolites generated from the two tracers. Neither of the putative oxidative metabolites, radiolabeled betaine or fluorobetaine, were detected in the cells at 2 h incubation, indicating oxidation of tracer choline and [^{18}F]FCH in the cultured cells to be negligible.

In hypoxic (1% O_2) conditions, the two choline tracers showed uptakes similar to those seen in normoxic conditions for incubation times up to 20 min (Figure 2). However, at 2hr, uptake of the choline tracers was found to be decreased approximately 50% in hypoxic cells relative to normoxic cells. In contrast with the results in normoxic cells, the major fraction of radioactivity in the aqueous fraction of hypoxic cells at early timepoints was contributed by nonmetabolized radiolabeled choline and [^{18}F]FCH (Figure 2). However, by 2 h post-incubation, 97% of the radioactivity was in the respective phosphorylated forms (Figure 2). Thus, hypoxia significantly slowed the rate of intracellular phosphorylation, decreased cellular retention (uptake), but did not decrease the ultimate extent of phosphorylation at later timepoints.

Proliferation rate was slightly slower in the hypoxic cells compared to normoxic cells (hypoxic doubling time = 2.2 ± 0.2 d versus normoxic doubling time = 1.8 ± 0.1 d). ATP concentration decreased by 30% and choline kinase activity decreased by 21% in hypoxic 9L glioma cells compared to 9L cells incubated under normoxic conditions (Table 2).

NIH-PA Author Manuscript

NIH-PA Author Manuscript

NIH-PA Author Manuscript

To further investigate the potential of the cells to oxidize [^{3}H]choline, incubations were performed in HEPES-Tris buffer at physiological concentration of 10 μM choline to promote higher uptake of [^{3}H]choline. After 1 h incubation with [^{3}H]choline, 11.0 ± 0.3% of the administered dose was found accumulated in the cells with no trace of [^{3}H]betaine. Analysis of the extracellular buffer showed a minute fraction of [^{3}H]betaine (0.3 ± 0.02%). As a negative control, the buffer incubated under similar conditions but without cells showed a complete absence of [^{3}H]betaine. These results show that phosphorylation is the major metabolic fate of [^{18}F]FCH and [^{3}H]choline in the cultured 9L glioma cells with relatively insignificant oxidation of tracers.

To investigate the potential role of dephosphorylation on the tracer kinetics of radiolabeled cholines, a pulse-chase experiment was performed. After the pulse of radiolabeled choline tracers for 2 h, moderate levels of radioactivity were washed out of the cells in successive 15 min incubations with medium lacking radioactivity (Figure 3). HPLC analysis of the incubation medium during the washout phase showed the radioactivity to be completely in the form of [^{14}C]choline and [^{18}F]FCH. Since it was shown that >99% or >97% of the intracellular radioactivity was in phosphorylated form in normoxic or hypoxic conditions, respectively, the clearance of radioactivity as [^{14}C]choline and [^{18}F]FCH demonstrated intracellular dephosphorylation and washout of the choline tracers from the cells. In normoxic conditions, [^{14}C]choline cleared the cells at a rate of 7.2% min^{-1}, whereas [^{18}F]FCH cleared at a slower rate of 4.3% min^{-1}. This suggested that phosphoryl-[^{18}F]FCH was more slowly dephosphorylated relative to [^{14}C]phosphocholine in normoxic 9L glioma cells . Washout rate was slightly decreased in hypoxic conditions for both [^{14}C]choline and [^{18}F]FCH.

Biodistribution and metabolism in 9L glioma rat model

Following bolus intravenous administration of [^{18}F]FCH and [^{14}C]choline , the plasma concentration of ^{18}F and ^{14}C-radioactivity decreased rapidly within the first 1.5 min post-injection (Figure 4). At 0.5 min, higher levels of ^{18}F-radioactivity were seen in plasma as compared to ^{14}C-radioactivity. No change was observed in the plasma concentration of radioactivity after 2 min for both tracers. HPLC analysis of plasma samples collected 2 min, 5 min and 20 min post-injection showed a decrease in the fraction of non-metabolized [^{14}C] choline and [^{18}F]FCH with time (post-injection) with a corresponding increase in [^{14}C]betaine and [^{18}F]fluorobetaine (Figure 5). The major tracer metabolites in plasma at 20 min post-injection were [^{14}C]betaine and [^{18}F]fluorobetaine. The rate of increase in the fraction of [^{14}C]betaine in plasma was higher than found for [^{18}F]fluorobetaine ($P<0.05$), suggesting somewhat slower oxidation of [^{18}F]FCH relative to choline.

Table 3 shows the biodistribution data for [^{14}C]choline and [^{18}F]FCH in the 9L tumor-bearing Fisher 344 rat model. The primary sites of uptake were found to be kidney and liver. Skeletal muscle, skin, L-intestine, lung and bone showed appreciable uptake of both tracers (arranged in order of decreasing uptake). No significant differences were seen in the amount of ^{18}F- and ^{14}C-radioactivity in the organs studied, suggesting biological similarity of [^{14}C]choline and [^{18}F]FCH. The amount of radioactivity remained nearly constant in most organs except kidney after 5 min post-injection. Kidney uptake decreased for both ^{18}F- and ^{14}C-radioactivity from 5 – 20 min, while urinary excretion increased to ~ 3% and ~ 6% of the injected dose of [^{14}C]choline and [^{18}F]FCH, respectively, at 20 min post-injection. HPLC analysis found >96 % of the radioactivity in urine to be in the form of nonmetabolized [^{14}C]choline and [^{18}F]FCH (Table 4). Thus, the higher urinary excretion with [^{18}F]FCH resulted from less tubular reabsorption of nonmetabolized tracer relative to [^{14}C]choline.

Table 5 shows the radioactivity distribution in aqueous and organic fractions in tumor and major tissues. Lung showed the highest fraction of lipid soluble choline metabolites of all tissues (37.4±7.0% at 20 min), followed by kidney (7.7±4.6%) and liver (5.2±0.9%). Lipophilic

NIH-PA Author Manuscript

NIH-PA Author Manuscript

NIH-PA Author Manuscript

metabolites increased from 5 to 20 min post-injection with corresponding decreases in aqueous soluble metabolites in all the major tissues except tumor. In all the tissues studied, moderately higher amounts of ^{14}C-radioactivity were seen in the lipophilic fractions as compared to ^{18}F-radioactivity, suggesting somewhat slower conversion of [^{18}F]FCH into lipid metabolites as compared to [^{14}C]choline.

In lung, HPLC analysis of the aqueous extract fraction (Table 6) showed significant decrease in nonmetabolized [^{14}C]choline and [^{18}F]FCH from 5 min to 20 min. This decrease accounted for the decrease in aqueous soluble radioactivity in lung with time. Similarly, in liver, decrease of radioactivity in aqueous fraction was primarily due to decrease in nonmetabolized [^{14}C] choline and [^{18}F]FCH. In contrast, the decrease of radioactivity in the aqueous fraction in kidney was determined by the washout of [^{14}C]betaine and [^{18}F]fluorobetaine. Metabolism of [^{14}C]choline and [^{18}F]FCH was comparable in liver except a lower amount of [^{18}F] fluorobetaine was seen relative to [^{14}C]betaine at 20 min post-administration. In addition there was a slight increase in [^{18}F]phosphofluorocholine from 5 min to 20 min post injection which was not seen for [^{14}C]phosphocholine.

In 9L tumor, hydrophilic metabolites dominated the fate of both [^{14}C]choline and [^{18}F]FCH, with 98% of radiolabel found in the aqueous phase at both timepoints (Table 6). Tumor:muscle and tumor:blood ratio decreased from 5 min to 20 min for both [^{14}C]choline and [^{18}F]FCH (Table 7). HPLC analysis of extracts of tumor showed major amount of radioactivity contributed by nonmetabolized [^{14}C]choline and [^{18}F]FCH. The fraction of nonmetabolized [^{18}F]FCH and [^{14}C]choline in tumor decreased from 5 min to 20 min. The fraction of radioactivity in the form of [^{14}C]betaine and [^{18}F]fluorobetaine was small but appreciable in tumor. This finding was in contrast to the negligible amount of [^{3}H]betaine production, low amount of nonmetabolized [^{14}C]choline and [^{18}F]FCH, and relatively high levels of phosphorylated forms of the tracers seen in cultured 9L glioma cells in normoxic conditions (Figure 2).

Discussion

Techniques for noninvasive imaging of cancer using PET are typically based on preferential binding or metabolic accumulation of a positron labeled tracer in cancer tissues. Elevated levels of choline uptake and choline kinase activity in neoplasms relative to normal tissues [2–4] have motivated the use of positron labeled cholines ([^{11}C]choline and [^{18}F]FCH) as cancer imaging agents [11–19]. Although the longer half-life of [^{18}F]FCH makes it more practical for distribution and clinical use, a thorough understanding of the biochemical handling of the fluorinated molecule has been lacking. The present findings on the uptake and metabolism of radiolabeled choline and FCH in cultured 9L glioma cells were in accordance with earlier reports showing similar biochemical handling of [^{18}F]FCH and [^{14}C]choline in cultured PC-3 prostate cancer cells [2]. Phosphorylation of choline and [^{18}F]FCH was the major metabolic process in 9L cells, with slow metabolism beyond their phosphorylated forms. Oxidative metabolism of [^{18}F]FCH and choline was a minor pathway. Incorporation of [^{3}H]choline and [^{18}F]FCH into membrane phospholipids of cultured cells was also found to be minimal for incubation periods up to 2h. Thus, phosphorylation of choline tracers was the major step of metabolism that accounted for accumulation of radioactivity in the cultured 9L cells.

The pulse-chase experiment showed higher washout rates for [^{14}C]choline than [^{18}F]FCH under both normoxic and hypoxic conditions. Since >95% of the radioactivity was in the form of the radiolabeled phosphorylated cholines in the normoxic and hypoxic cells after 2h incubation, washout of radioactivity in the pulse chase experiment indicated that dephosphorylation of intracellular [^{14}C]phosphocholine (and phosphoryl-[^{18}F]FCH) is a small but significant process. The implied slower washout rate of [^{18}F]FCH than [^{14}C]choline in

NIH-PA Author Manuscript

NIH-PA Author Manuscript

NIH-PA Author Manuscript

both normoxic and hypoxic conditions may result from the effects of the radiofluorine atom on phosphatase-catalyzed dephosphorylation rate or transmembrane transport.

In contrast to the observations in cultured cancer cells, both [^{18}F]FCH and [^{14}C]choline showed extensive oxidation in rats. Rapid clearance of the choline tracers from the bloodstream was observed, while plasma levels of their oxidative metabolites, [^{18}F]fluorobetaine and [^{14}C] betaine, respectively, increased over the first 20 min post-injection. These results are similar to earlier reports of choline uptake and metabolism in humans and rats (using [*methyl*-^{11}C] choline) [20] and guinea pigs (using [methyl-^{3}H]choline) [25]. The major metabolite of [^{11}C] choline in human plasma was also identified as [^{11}C]betaine [20]. Decay-corrected plasma levels of [^{11}C]betaine increased over the first 20 min following intravenous bolus administration of [^{11}C]choline. Studies with [*methyl*-^{3}H]choline in guinea pigs showed the half-life of choline in plasma to be less than 1 min and the rapid removal of choline was accomplished mainly by kidney and liver.

The high accumulation of choline radiotracers in kidney and liver reflects the important role of these organs in choline metabolism in the body. Kidney and liver are known to be the major sites for oxidation of choline to betaine [20,25]. Betaine is an important donor of methyl groups for formation of methionine [26] which is used for the synthesis of S-adenosyl methionine. In the kidney, betaine serves as an osmolyte [27]. Some betaine is also transported from the kidney to other organs for use as an osmolyte or methyl donor. The rapid uptake and clearance of the choline tracers in liver and kidney indicate the importance of tissue perfusion on their biodistribution.

There was observed a trend toward higher urinary excretion of [^{18}F]FCH relative to [^{14}C] choline in the rat model but the difference was not statistically significant. Since the majority of radiolabel in the urine was in the form of nonmetabolized [^{18}F]FCH, the data suggest less tubular reabsorption of [^{18}F]FCH relative to choline. Interestingly, the early urinary excretion of [^{11}C]choline in human patients appears to be negligible [9], while excretion of [^{18}F]FCH is significant within 10 min post-administration [2,11], suggesting a species difference in the renal handling of [^{18}F]FCH relative to radiolabeled choline.

In lung, the fractions of radioactivity that were found as organic soluble metabolites of [^{18}F] FCH and [^{14}C]choline were nearly an order of magnitude higher than those found in liver and kidney. Although these fractions were not chemically identified, it is assumed that they represent incorporation of radioactivity into phospholipid metabolites, including phosphatidylcholine. The major fate of exogenous choline in lung tissue was previously shown to be incorporation into pulmonary surfactant composed of predominantly phosphatidylcholine [28]. The present data are consistent with this report. The conversion of [^{14}C]phosphocholine and phosphoryl-[^{18}F]fluorocholine to ^{14}C- and ^{18}F-labeled phospholipids, respectively, is suggested by the increases in the organic soluble radioactivity fraction over the 5 to 20 min interval for both [^{14}C]choline and [^{18}F]FCH, while levels of their corresponding phosphorylated metabolites were in decline. Lipid incorporation of [^{14}C]choline in lung was 1.5 fold that of [^{18}F]FCH (37.4±7.0% versus 22.3±2.8% at 20 min post-injection), suggesting an affect of the fluorine atom to cause a significant slowing of conversion throughout the Kennedy pathway for fluorocholine beyond the phosphorylation step. Lower lipid incorporation was also observed in liver, kidney and tumor for [^{18}F]FCH relative to [^{14}C] choline, but the quantitative importance of these differences is less in these tissues considering the lower levels (<8%) of radioactivity associated with the lipid fraction.

The uptake of choline radiotracers by muscle was low; however an increase in uptake was seen over the first 20 min post-injection. Since greater than 50% of plasma radioactivity is in the form of radiolabeled betaine after 5 min post-injection, the increased amount of radioactivity

NIH-PA Author Manuscript

NIH-PA Author Manuscript

NIH-PA Author Manuscript

in muscle may reflect uptake of betaine metabolites in muscle. Also, synthesis of phosphoglycerides involving the CDP-choline pathway has been reported in muscle which could support accumulation of tracers in muscles [29,30].

Uptake of both tracers in subcutaneous 9L tumor was low relative to kidney, liver and lung, with no differences noted between [^{18}F]FCH and [^{14}C]choline. Both [^{14}C]choline and [^{18}F]FCH were taken up but very slowly metabolized to their oxidized or phosphorylated forms. The uptake was dominated by choline radiotracers in their nonmetabolized form. Bearing in mind that cultured 9L cells showed insignificant oxidation of choline tracers, the source of radiolabeled betaines found in *in vivo* tumors may be extratumoral. The finding of low levels of phosphorylated radiolabeled tracers in subcutaneous 9L tumors can result from slower rate of phosphorylation of tracers in hypoxic 9L tumors. We have recently shown that hypoxia profoundly decreased choline transport and phosphorylation in hypoxic prostate cancer cells (PC-3 and LNCaP) [31]. Inhibition of choline phosphorylation due to ATP depletion was also reported in hypoxic HL-1 cardiomyocytes [32] and AICAr treated hepatocytes [33]. The present results with cultured 9L glioma cells under hypoxia (1% O_2) showed a 20% decrease in choline kinase activity and 30% decrease in ATP concentration as compared to 9L glioma cells under normoxic conditions (21% O_2) (Table 2). Furthermore, a markedly lower rate of phosphorylation of choline tracers was seen in cultured 9L glioma cells under hypoxia (1% O_2) as compared to normoxic cells (21% O_2) with majority of the choline radiotracers in their nonmetabolized form (Figure 2). The pulse-chase experiment showed higher washout rates from for [^{14}C]choline than [^{18}F]FCH from hypoxic cultured 9L cells. It is suggested that hypoxia can explain the low levels of choline phosphorylation in the 9L glioma tumor model. This notion is further supported by earlier reports by Koch et al. [21] demonstrating extreme levels of hypoxia (median pO_2 value 5.5mm Hg) resulting from low perfusion in the same subcutaneous 9L tumor. These results of choline tracer studies with this experimental model may best interpolate to human tumors that are characteristically hypoxic. It follows that the utility of choline tracers in the clinical setting may be impacted by tumor hypoxia. Tumors that are hypoxic may exhibit low uptake of choline based tracers as governed by poor delivery (perfusion), increased efflux of nonmetabolized tracer and decreased metabolic trapping (phosphorylation). Thus, interpretations of clinical PET images with choline radiotracers should bear in mind that choline tracer uptake may underestimate tumor proliferation (or viability) in hypoxic tumor regions.

Conclusions

Comparable transport and metabolic characteristics of [^{18}F]FCH and [^{14}C]- or [^{3}H]-choline are evident in both cultured 9L cells and in the subcutaneous 9L tumor bearing Fisher rat model. [^{18}F]FCH mimics radiolabeled choline as a biochemical tracer, although metabolic rates to both lipid and oxidative metabolites were moderately attenuated for [^{18}F]FCH relative to [^{14}C]choline as implied by differences in distribution of ^{18}F- and ^{14}C-radioactivity in metabolite fractions. The enhanced renal excretion of [^{18}F]FCH relative to radiolabeled choline reflects incomplete tubular reabsorption of the tracer in its nonmetabolized form. Nevertheless, it is concluded that [^{18}F]FCH may serve as a useful radiotracer for noninvasive assessment of choline uptake and metabolism in *in vivo* studies. The finding of dramatically reduced choline tracer phosphorylation in hypoxic 9L glioma cells, corroborating earlier findings from this laboratory in PC-3 cancer cells, suggests that tumor hypoxia may profoundly lower choline metabolic trapping in cancer cells. Thus, choline tracer retention may be related to tumor oxygenation status through effects on choline kinase activity. This effect has clear implications for interpretation of clinical PET images with choline radiotracers; tumor proliferation (or viability) may be underestimated in hypoxic tumor regions.

NIH-PA Author Manuscript

NIH-PA Author Manuscript

NIH-PA Author Manuscript

Acknowledgements

The work was funded in part by NIH (RO1 CA108620, R01 HL-63371) and the INGEN Program of Indiana University School of Medicine (IUSM), a grant from the Lilly Endowment. The authors thank Dr. Frank A. Witzmann and Seokmin Hong in Department of Cellular & Integrative Physiology, IUSM for their help in LCMS quantification of [^{19}F]FCH.

The work was funded in part by NIH (RO1 CA108620, R01 HL-63371) and the INGEN Program of Indiana University School of Medicine, a grant from the Lilly Endowment.

References

1. Gillies RJ, Morse DL. In vivo magnetic resonance spectroscopy in cancer. Annu Rev Biomed Eng 2005;7:287–326. [PubMed: 16004573]
2. DeGrado TR, Coleman RE, Wang S, et al. Synthesis and evaluation of ^{18}F-labeled choline as an oncologic tracer for positron emission tomography: initial findings in prostate cancer. Cancer Res 2001;61(1):110–117. [PubMed: 11196147]
3. Katz-Brull R, Seger D, Rivenson-Segal D, Rushkin E, Degani H. Metabolic markers of breast cancer: enhanced choline metabolism and reduced choline-ether-phospholipid synthesis. Cancer Res 2002;62 (7):1966–1970. [PubMed: 11929812]
4. Katz-Brull R, Degani H. Kinetics of choline transport and phosphorylation in human breast cancer cells: NMR application of the zero trans method. Anticancer Res 1996;16(3B):1375–1380. [PubMed: 8694504]
5. Hara T, Kosaka N, Kishi H. Development of ^{18}F-fluoroethylcholine for cancer imaging with PET: synthesis, biochemistry, and prostate cancer imaging. J Nucl Med 2002;43(2):187–199. [PubMed: 11850483]
6. Ramirez de Molina A, Rodriguez-Gonzalez A, Gutierrez R, Martinez-Pineiro L, et al. Overexpression of choline kinase is a frequent feature in human tumor-derived cell lines and in lung, prostate, and colorectal human cancers. Biochem Biophys Res Commun 2002;296(3):580–583. [PubMed: 12176020]
7. Shinoura N, Nishijima M, Hara T, et al. Brain tumors: detection with C-11 choline PET. Radiology 1997;202(2):497–503. [PubMed: 9015080]
8. Hara T, Kosaka N, Shinoura N, Kondo T. PET imaging of brain tumor with [methyl-^{11}C]choline. J Nucl Med 1997;38(6):842–847. [PubMed: 9189127]
9. Hara T, Kosaka N, Kishi H. PET imaging of prostate cancer using carbon-11-choline. J Nucl Med 1998;39(6):990–995. [PubMed: 9627331]
10. Hara M. Clinical studies on cefoperazone and polymyxin B for the treatment of infections in patients with hematological malignancies. Jpn J Antibiot 1987;40(9):1639–1643. [PubMed: 2826837]
11. DeGrado TR, Baldwin SW, Wang S, et al. Synthesis and evaluation of ^{18}F-labeled choline analogs as oncologic PET tracers. J Nucl Med 2001;42(12):1805–1814. [PubMed: 11752077]
12. Talbot JN, Gutman F, Fartoux L, et al. PET/CT in patients with hepatocellular carcinoma using [^{18}F]fluorocholine: preliminary comparison with [^{18}F]FDG PET/CT. Eur J Nucl Med Mol Imaging. 2006 Jun 27;
13. Kwee SA, Wei H, Sesterhenn I, Yun D, Coel MN. Localization of Primary Prostate Cancer with Dual-Phase ^{18}F-Fluorocholine PET. J Nucl Med 2006;47(2):262–269. [PubMed: 16455632]
14. Heinisch M, Dirisamer A, Loidl W, et al. Positron emission tomography/computed tomography with F-18 fluorocholine for restaging of prostate cancer patients: meaningful at PSA < 5 ng/ml? Mol Imaging Biol 2006;8(1):43–48. [PubMed: 16315004]
15. Cimitan M, Bortolus R, Morassut S, et al. [^{18}F] fluorocholine PET/CT imaging for the detection of recurrent prostate cancer at PSA relapse: experience in 100 consecutive patients. Eur J Nucl Med Mol Imaging. 2006 July 25;
16. Schmid DT, John H, Zweifel R, et al. Fluorocholine PET/CT in patients with prostate cancer: initial experience. Radiology 2005;235(2):623–628. [PubMed: 15858102]
17. Kwee SA, Coel MN, Lim J, Ko JP. Prostate cancer localization with fluorine-18 fluorocholine positron emission tomography. J Urol 2005;173(1):252–255. [PubMed: 15592091]

NIH-PA Author Manuscript

NIH-PA Author Manuscript

NIH-PA Author Manuscript

18. Kwee SA, Coel MN, Lim J, Ko JP. Combined use of F-18 fluorocholine positron emission tomography and magnetic resonance spectroscopy for brain tumor evaluation. J Neuroimaging 2004;14 (3):285–289. [PubMed: 15228773]
19. Price DT, Coleman RE, Liao RP, Robertson CN, Polascik TJ, DeGrado TR. Comparison of [^{18}F] fluorocholine and [^{18}F]fluorodeoxyglucose for positron emission tomography of androgen dependent and androgen independent prostate cancer. J Urol 2002;168(1):273–280. [PubMed: 12050555]
20. Roivainen A, Forsback S, Gronroos T, et al. Blood metabolism of [methyl-^{11}C]choline; implications for in vivo imaging with positron emission tomography. Eur J Nucl Med 2000;27(1):25–32. [PubMed: 10654143]
21. Timothy, Jenkins W.; Evans, Sydney M.; Koch, Cameron J. Hypoxia and necrosis in rat 9L glioma and morris 7777 hepatoma tumors: comparative measurements using EF5 binding and the eppendorf needle electrode. Int J Radiation Oncology Biol Phys 2000;46 (4):1005–1017.
22. Liu L, Cash TP, Jones RG, Keith B, Thompson CB, Simon MC. Hypoxia-induced energy stress regulates mRNA translation and cell growth. Mol Cell 2006;21:521–531. [PubMed: 16483933]
23. Lamprecht, HU.; Trautschold, W. Determination of ATP by hexokinase and glucose-6-phosphate dehydrogenase. In: Bergmeyer, Hans Ulrich, editor. Methods Enzym Anal. 2. New York, U.S.A: Academic Press; 1974. p. 2101-2110.
24. Ishidate K, Nakazawa Y. Choline/ethanolamine kinase from rat kidney. Methods in Enzymology 1992;209:121–134. [PubMed: 1323025]
25. Haubrich DR, Wang PF, Wedeking PW. Distribution and metabolism of intravenously administered choline[methyl- 3-H] and synthesis in vivo of acetylcholine in various tissues of guinea pigs. J Pharmacol Exp Ther 1975;193(1):246–255. [PubMed: 1133767]
26. Finkelstein JD, Martin JJ, Harris BJ, Kyle WE. Regulation of the betaine content of rat liver. Arch Biochem Biophys 1982;218 (1):169–173. [PubMed: 7149724]
27. Garcia-Perez A, Burg MB. Role of organic osmolytes in adaptation of renal cells to high osmolality. J Membr Biol 1991;119:1–13. [PubMed: 1901090]
28. Rooney SA, Young SL, Mendelson CR. Molecular and cellular processing of lung surfactant. Faseb J 1994;8(12):957–967. [PubMed: 8088461]
29. Pennington RJ, Worsfold M. Biosynthesis of lecithin by skeletal muscle. Biochim Biophys Acta 1969;176(4):774–782. [PubMed: 5797090]
30. Shamgar FA, Collins FD. Incorporation of ortho[^{32}P]phosphate into phosphatidylcholines and phosphatidylethanolamines in rat skeletal muscle. Biochim Biophys Acta 1975;409(1):104–115. [PubMed: 1182189]
31. Hara T, Bansal A, DeGrado TR. Effect of Hypoxia on Uptake of [*methyl*-^{3}H]choline, [1-^{14}C]acetate and [^{18}F]FDG in cultured prostate cancer cells. Nucl Med Biol 2006 Nov;33(8):977–84. [PubMed: 17127170]
32. Sarri E, Garcia-Dorado D, Abellan A, Soler-Soler J. Effects of hypoxia, glucose deprivation and acidosis on phosphatidylcholine synthesis in HL-1 cardiomyocytes. CTP:phosphocholine cytidylyltransferase activity correlates with sarcolemmal disruption. Biochem J 2006 Feb 15;394(1): 325–34. [PubMed: 16236026]
33. Jacobs RL, Lingrell S, Dyck JR, Vance DE. Inhibition of Hepatic Phosphatidylcholine Synthesis by 5-Aminoimidazole-4-carboxamide-1-beta-4-ribofuranoside Is Independent of AMP-activated Protein Kinase Activation. J Biol Chem 2007 Feb 16;282(7):4516–23. [PubMed: 17179149]

NIH-PA Author Manuscript

NIH-PA Author Manuscript

NIH-PA Author Manuscript

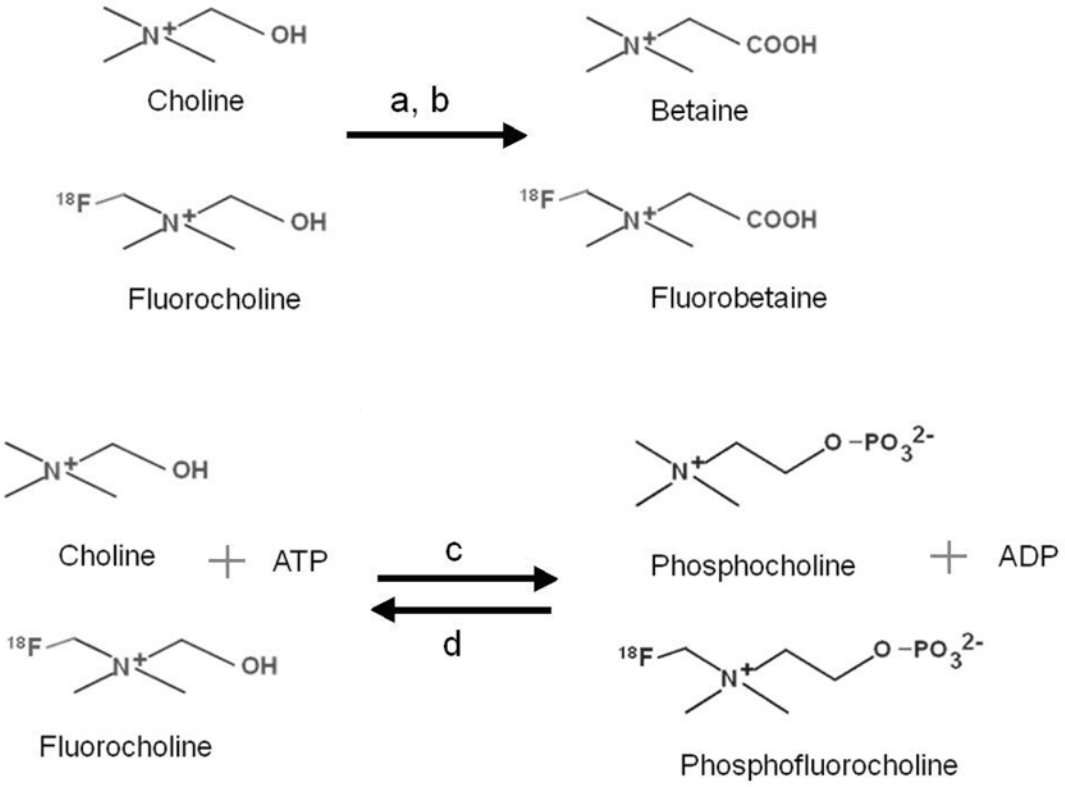

Figure 1.
Chemical structures of tracers showing oxidation of choline and fluorocholine by (a) choline dehydrogenase and (b) betaine-aldehyde dehygrdogenase, phosphorylation by (c) choline kinase and dephosphorylation by (d) phosphatase.

NIH-PA Author Manuscript
NIH-PA Author Manuscript
NIH-PA Author Manuscript

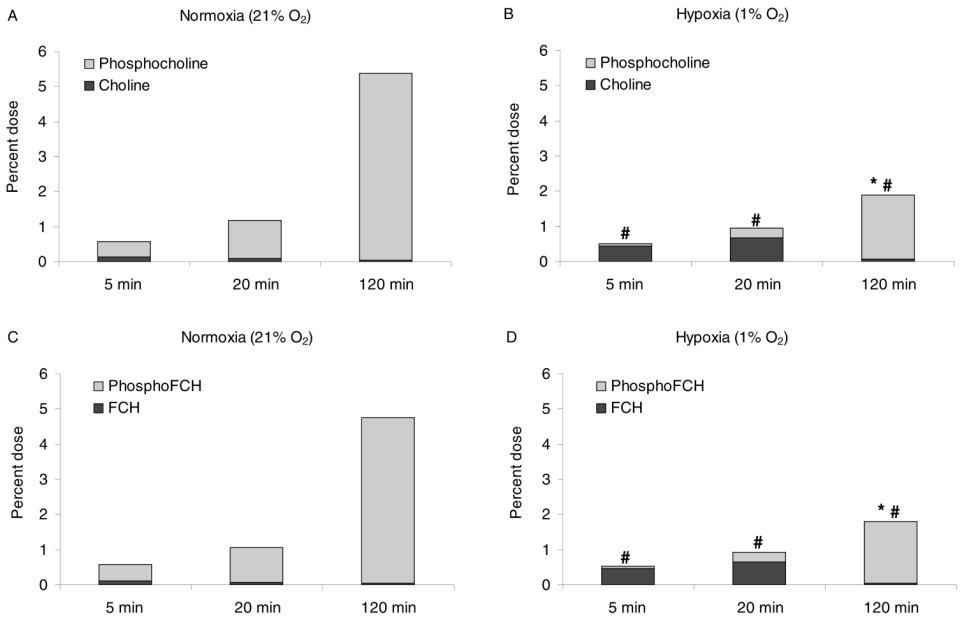

Figure 2.

Uptake and metabolism of radiolabeled choline and [^{18}F]FCH in cultured 9L glioma cells as function of oxygenation status and incubation period. (a) radiolabeled choline (24h normoxia), (b) radiolabeled choline (24h hypoxia), (c) [^{18}F]FCH (24h normoxia), and (d) [^{18}F]FCH (24h hypoxia). Values are shown as % administered dose per 10^6 cells (mean ± standard deviation, n=3). * $p < 0.05$ versus total uptake in normoxic condition using unpaired t-test. $^{\#}$ $p < 0.05$ versus metabolite fraction in normoxic condition using unpaired t-test.

NIH-PA Author Manuscript

NIH-PA Author Manuscript

NIH-PA Author Manuscript

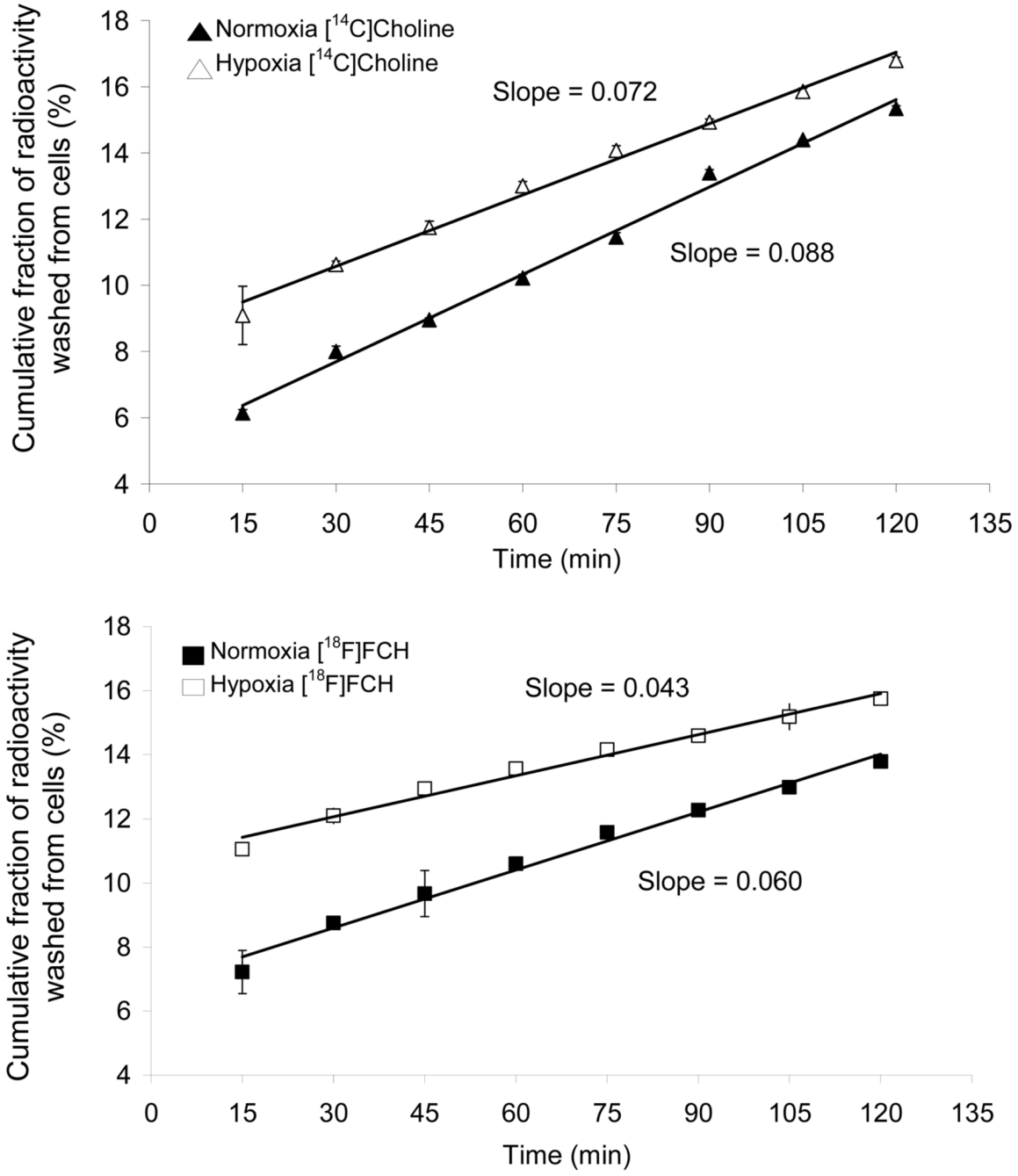

Figure 3.

Efflux of trapped ^{14}C-radioactivity (a) and [^{18}F]F-radioactivity (b) from normoxic and hypoxic cells upon successive washing after incubating the cells for 2 h with [^{14}C]choline and [^{18}F] FCH under normoxic (21% O_2) and hypoxic (1% O_2) condition. Slopes of linear fits to the data are shown. Y –axis shows fraction of % administered dose/10^6 cells washed out into the medium (mean ± standard deviation, n=3).

NIH-PA Author Manuscript
NIH-PA Author Manuscript
NIH-PA Author Manuscript

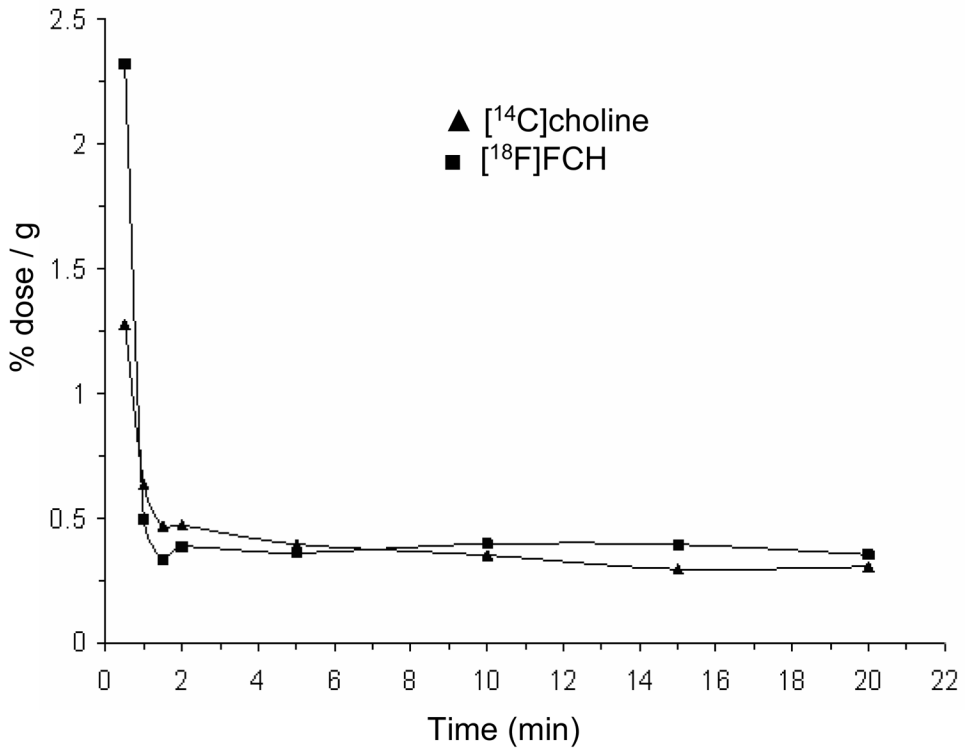

Figure 4.
Time-course of plasma radioactivity concentration (dose/g) for [^{18}F]FCH (squares) and [^{14}C] choline (triangles) (n=4).

NIH-PA Author Manuscript

NIH-PA Author Manuscript

NIH-PA Author Manuscript

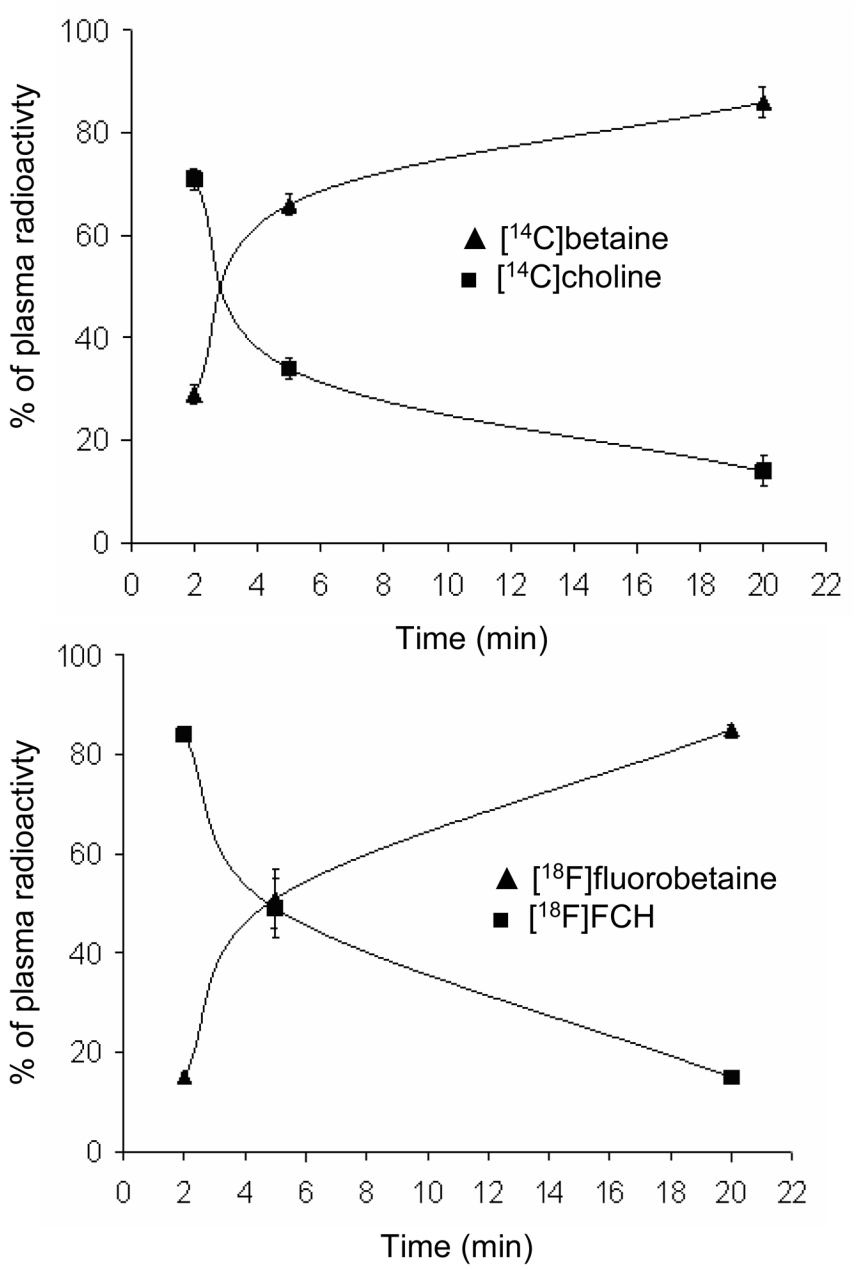

Figure 5.
Change in metabolites of (a) [^{14}C]choline and (b) [^{18}F]FCH in plasma at different time points post-injection (n=4).

NIH-PA Author Manuscript

NIH-PA Author Manuscript

NIH-PA Author Manuscript

Table 1

Radioactive metabolites of [^{3}H]choline and [^{18}F]FCH in cultured 9L glioma cells at 2h incubation.

	Metabolite	Radioactivity distribution (%)	
		^{3}H	^{18}F
Total		5.69±0.31	6.64±0.67
Organic Phase		1.13±0.24	0.86±0.17
Aqueous Phase	Choline	0.015±0.018	0.045±0.027
	Phosphocholine	4.55±0.13	5.71±0.17
	Total	4.56±0.24	5.76±0.17

Values are mean ± standard deviation for N=3; Paired t-test was done compare values for [^{3}H]choline and [^{18}F]FCH.

NIH-PA Author Manuscript

NIH-PA Author Manuscript

NIH-PA Author Manuscript

Table 2

ATP level and choline kinase (CK) activity in cultured 9L glioma cells under 24h normoxia and hypoxia

Condition (24h)	ATP (nmol/mg protein)	CK activity (pmol/min/mg)
Normoxia	17.2 ± 0.5	113.3 ± 6.8
Hypoxia	12.0 ± 0.4*	92.0 ± 7.9*

*P value < 0.05 versus normoxia using unpaired t-test.

Values are mean ± standard deviation for N=3

NIH-PA Author Manuscript
NIH-PA Author Manuscript
NIH-PA Author Manuscript

Table 3

Biodistribution of [^{14}C]choline and [^{18}F]FCH in 9L glioma-bearing Fischer rats

Organ/tissue	Time post-injection (min)	Uptake			
		^{14}C	^{14}C	^{18}F	^{18}F
		Dose/g (%)	Dose (%)	Dose/g (%)	Dose (%)
Blood	5	0.18±0.10	1.7±1.3	0.27±0.08	3.1±0.8
	20	0.13±0.10	1.7±1.1	0.25±0.09	3.2±1.2
Bone	5	0.18±0.13	1.03±0.70	0.17±0.1	1.05±0.71
	20	0.10±0.04	1.05±0.04	0.14±0.04	1.06±0.04
Brain	5	0.07±0.03	0.04±0.02	0.05±0.02	0.03±0.01
	20	0.04±0.01	0.03±0.01	0.04±0.01	0.02±0.01
Colon	5	0.53±0.17	-	0.47±0.07	-
	20	0.49±0.12	-	0.53±0.16	-
Heart	5	0.47±0.16	0.29±0.07	0.45±0.16	0.27±0.07
	20	0.36±0.12	0.24±0.08	0.47±0.15	0.31±0.09
Kidney	5	15.9±7.2	24.7±9.8	15.57±6.52	24.1±8.6
	20	5.6±1.6*	9.4±3.3*	7.27±2.15*	12.2±4.2*
L-intestine	5	1.2±0.7	2.6±1.3	0.97±0.39	2.1±0.8
	20	1.2±0.4	2.6±0.8	1.07±0.37	2.4±0.7
Liver	5	3.1±1.4	24.6±9.8	2.61±0.84	20.9±5.3
	20	3.9±0.81	33.4±6.6	3.16±0.68	27.0±5.6
Lung	5	1.9±0.9	1.9±1.0	1.65±0.92	1.6±1.0
	20	1.05±0.31	1.1±0.3	1.1±0.35	1.1±0.3
Plasma	5	0.40±0.10	-	0.4±0.12	-
	20	0.44±0.27	-	0.37±0.07	-
Prostate	5	1.2±0.6	0.01±0.01	1.11±0.62	0.01±0.01
	20	1.0±0.6	0.01±0.01	1.34±0.89	0.01±0.01
Skeletal muscle	5	0.13±0.09	11.7±8.8	0.11±0.06	10.03±6.7
	20	0.18 ±0.05*	17.5±4.4*	0.21±0.08*	20.2±6.5*
Skin	5	0.43±0.31	12.7±8.6	0.38±0.21	11.4±5.5
	20	0.30±0.18	10.0±5.7	0.37±0.21	11.9±6.4
Spleen	5	0.74±0.19	0.35±0.07	0.79±0.15	0.37±0.07
	20	0.42±0.07	0.21±0.05	0.72±0.23	0.36±0.11
Tumor	5	0.76±0.48	-	0.69±0.41	
	20	0.19±0.12	-	0.22±0.10	-
Urine	5	-	1.5±0.2	-	2.4±0.3
	20	-	3.4±1.4*	-	6.4±2.5*

*P value < 0.05 versus 5 min using unpaired t-test

Values are mean ± standard deviation for N=4

NIH-PA Author Manuscript

NIH-PA Author Manuscript

NIH-PA Author Manuscript

Table 4

Urinary excretion of [^{14}C]choline and [^{18}F]FCH metabolites

Metabolite	Radioactivity (% dose) at 5 min post-injection		Radioactivity (% dose) at 20 min post-injection	
	^{14}C	^{18}F	^{14}C	^{18}F
Betaine	0.03±0.01	0.05±0.01	0.2±0.05	0.4±0.06*
Choline	1.4±0.4	2.4±0.9	3.2±0.8	6.1±1.3*
Phosphocholine	n.d.	n.d.	n.d.	n.d.

*P value < 0.05 versus ^{14}C using paired t-test; n.d. - not detected

Values are mean ± standard deviation for N=4

NIH-PA Author Manuscript
NIH-PA Author Manuscript
NIH-PA Author Manuscript

Table 5

Distribution of radioactivity in aqueous and organic fractions of tissue extracts

Organ	^{18}F	^{18}F	^{14}C	^{14}C
	5 min	20 min	5 min	20 min
	Aqueous fraction (%)	Aqueous fraction (%)	Aqueous fraction (%)	Aqueous Fraction (%)
Lung	94.0±1.1	77.7±2.8*	87.3±2.8#	62.6±7.0*#
Liver	99.4±0.2	97.4±0.6	98.7±0.7	94.8±0.9#
Kidney	99.4±0.3	96.7±2.2	99.1±0.3	92.3±4.6*#
Tumor	98.4±1.3	99.1±0.3	97.9±0.9	98.2± 1.4
	Organic fraction (%)	Organic fraction (%)	Organic fraction (%)	Organic fraction (%)
Lung	5.9±1.1	22.3±2.8*	12.7±2.8#	37.4±7.0*#
Liver	0.6±0.2	2.6±0.6*	1.3±0.7	5.2±0.9*#
Kidney	0.6±0.3	3.3±2.2	0.9±0.3	7.7±4.6*#
Tumor	1.6±1.3	0.9±0.3	2.1±0.9	1.8±1.4

*P value < 0.05 versus 5 min using unpaired t-test;

#P value < 0.05 versus ^{18}F using paired t-test. Values are mean ± standard deviation for N=4

NIH-PA Author Manuscript

NIH-PA Author Manuscript

NIH-PA Author Manuscript

Table 6

HPLC analysis of hydrophilic metabolites of [^{18}F]FCH and [^{14}C]choline

Organ/Tissue	Metabolite	Time (min)	Radioactivity (% dose / g)	
			^{14}C	^{18}F
Kidney	Betaine	5	12.85± 6.25	11.25± 3.57
		20	4.23±0.81*	4.72±1.16*
	Choline	5	1.85±1.35	3.56±3.43
		20	0.30±0.26	0.57±0.55
	Phosphocholine	5	1.02±0.45	0.98±0.47
		20	0.61±0.37	1.77±0.73*
Liver	Betaine	5	2.10±1.06	1.40±0.52
		20	2.73±0.77	1.27±0.44*#
	Choline	5	0.20±0.12	0.31±0.20
		20	0.08±0.02	0.10±0.08
	Phosphocholine	5	0.74±0.22	0.87±0.12
		20	0.89±0.56	1.71±0.48*
Lung	Betaine	5	0.47±0.31	0.11±0.04
		20	0.18 ±0.05	0.12±0.03
	Choline	5	0.36±0.17	0.67±0.37
		20	0.09±0.03*	0.15±0.05*
	Phosphocholine	5	0.87±0.49	0.78±0.48
		20	0.39±0.17	0.58±0.21
Tumor	Betaine	5	0.10±0.07	0.020±0.01
		20	0.04±0.02	0.040±0.02
	Choline	5	0.65±0.40	0.60±0.36
		20	0.090±0.08*	0.12±0.07*
	Phosphocholine	5	n.d.	0.05±0.03
		20	0.05±0.03	0.06±0.04

*P value < 0.05 versus 5 min using unpaired t-test;

#P value < 0.05 versus ^{14}C using paired t-test; n.d.- not detected Values are mean ± standard deviation for N=4

NIH-PA Author Manuscript

NIH-PA Author Manuscript

NIH-PA Author Manuscript

Table 7

Tumor:background ratio of [^{14}C]choline and [^{18}F]FCH in 9L glioma-bearing Fischer rats

	Time post- injection (min)	^{14}C	^{18}F
Tumor:Blood	5	4.22±0.84	2.55±0.66
	20	1.46±1*	0.88±0.58*
Tumor:Muscle	5	5.85±0.94	6.27±0.81
	20	1.05±0.69*	1.05±0.59*

* P value < 0.05 versus 5 min using unpaired t-test

Values are mean ± standard deviation for N=4